SAND2023-06081C

**Proceedings of the ASME 2023 17th International Conference on Energy Sustainability**
**ES2023**
**July 10-12, 2023, Washington, DC**

# ES2023-107547

## CONTROLS AND OPERATIONAL STRATEGY FOR GEN 3 PARTICLE PILOT PLANT

**Hendrik F. Laubscher**
Sandia National Laboratories
Albuquerque, NM

**Luis G. Maldonado**
Sandia National Laboratories
Albuquerque, NM

**Francisco Alvarez**
Sandia National Laboratories
Albuquerque, NM

**Luke P. McLaughlin**
Sandia National Laboratories
Albuquerque, NM

**Nathaniel R. Schroeder**
Sandia National Laboratories
Albuquerque, NM

**Kevin J. Albrecht**
Sandia National Laboratories
Albuquerque, NM

**Jeremy N.I. Sment**
Sandia National Laboratories
Albuquerque, NM

**Kaden Plewe**
The University of Texas at Austin
Austin, TX

## ABSTRACT

*A comprehensive control strategy is necessary to safely and effectively operate particle based concentrating solar power (CSP) technologies. Particle based CSP with thermal energy storage (TES) is an emerging technology with potential to decarbonize power and process heat applications. The high-temperature nature of particle based CSP technologies and daily solar transients present challenges for system control to prevent equipment damage and ensure operator safety. An operational controls strategy for a tower based particle CSP system during steady state and transient conditions with safety interlocks is described in this paper. Control of a solar heated particle recirculation loop, TES, and a supercritical carbon dioxide ($sCO_2$) cooling loop designed to reject 1 MW of thermal power are considered and associated operational limitations and their influence on control strategy are discussed.*

Keywords: Supercritical carbon dioxide, concentrating solar power, CSP, renewable energy, Generation 3 CSP

## NOMENCLATURE

| | |
|---|---|
| $\dot{m}$ | Mass flow rate of particles through receiver, $kg/s$ |
| $T_s$ | Lumped temperature state in receiver model, °C |
| $T_{s,in}$ | Receiver particle inlet temperature, °C |
| $T_\infty$ | Ambient temperature, $°C$ |
| $h_\infty$ | Ambient heat transfer coefficient around receiver, $W/m^2K$ |
| $G_{solar}$ | Solar irradiation received by falling particle curtain, $W$ |
| $c_{p,s}$ | Particle specific heat, $J/kgK$ |
| $\rho_s$ | Bulk falling particle curtain density, $kg/m^3$ |
| $V_s$ | Volume of falling particle curtain, $m^3$ |
| $\alpha_s$ | Solar absorptivity of falling particle curtain |
| $\epsilon_s$ | Falling particle curtain emissivity |
| $\sigma$ | Stephan-Boltzmann constant, $W/m^2K^4$ |
| $A_s$ | Surface area of falling particle curtain, $m^2$ |
| $B_w$ | State-space disturbance input matrix |
| $C_z$ | State-space state measurement matrix |
| $D_{zw}$ | State-space disturbance measurement matrix |
| $w$ | Disturbance vector for receiver model |
| $z$ | Measured receiver variables |
| $G_p$ | Receiver plant transfer function symbol |
| $K_p$ | Proportional feedback controller for receiver |
| $K_{uw}$ | Feedforward controller for receiver |
| $T_{wz}$ | Transfer function from disturbance variables to measured outputs in the receiver |
| $e$ | Particle temperature setpoint error, $°C$ |
| $F^0$ | Linearized system reference time derivative, $°C/s$ |
| $F$ | Falling particle receiver lumped model time derivative, $°C/s$ |
| $\beta$ | Partial derivative of $F$ with respect to $T_s$, $s^{-1}$ |
| $\gamma$ | Partial derivative of $F$ with respect to $T_\infty$, $s^{-1}$ |
| $\zeta$ | Partial derivative of $F$ with respect to $\dot{m}$, °C/$kg$ |
| $\theta$ | Partial derivative of $F$ with respect to $T_{s,in}$, $s^{-1}$ |
| $\psi$ | Partial derivative of $F$ with respect to $G_{solar}$, °C/$J$ |




Sandia National Laboratories is a multimission laboratory managed and operated by National Technology & Engineering Solutions of Sandia, LLC, a wholly owned subsidiary of Honeywell International Inc., for the U.S. Department of Energy's National Nuclear Security Administration under contract DE-NA0003525.

## 1 INTRODUCTION

Automation of controls for the Generation 3 Particle Pilot Plant (G3P3) is an area where many operational uncertainties remain. Up to 1000 hours' worth of operational experimental testing is planned to occur after the construction and commissioning of the pilot facility is completed. Current experience at the National Solar Thermal Test Facility (NSTTF) in the operation of particle-heated $sCO_2$ thermal loops consist of testing the 100 $kW_{th}$ SunShot National Laboratory Multiyear Partnership (SuNLaMP) heat exchanger and various smaller heat exchangers in the 20 $kW_{th}$ test stand at the NSTTF [1], [2]. Both of these particle-$sCO_2$ thermal loops were extensively tested (collectively >500 hours) under electrically heated conditions. Control strategies for transient and steady state operational conditions were developed during the above-mentioned studies. The simplified controllable nature of electricity as the primary energy input for the heat addition in the thermal loop reduced the dependent variables in the process which significantly simplified the controls challenge. Limited on-sun operational test experience exists for this style of power cycle fluid, $sCO_2$, and primary energy carrier, ceramic particles.

The development of the control strategies and philosophy for G3P3 will combine the aspects of direct solar input as the primary energy source, integration of a TES and continuous heat rejection with an $sCO_2$ loop. The individual component control strategies have been developed and tested, but the full system has not been demonstrated. The refinement, development and optimization of controls for the fully integrated on-sun system will be discussed in this paper.

The falling particle receiver (FPR) which collects the solar thermal energy has been extensively tested and characterized at the NSTTF [3], [4], [5]. In order to control receiver outlet temperature, two variables can be manipulated, namely receiver mass flow rate and solar heat flux input. An outlet temperature control strategy which uses PID controller to modulate the mass flow rate into the receiver has been demonstrated in previous on-sun experiments [5]. A complementary dynamic feedforward controller that is designed specifically to perturb the falling particle mass flow rate to reject disturbances in solar flux, ambient temperature, and particle inlet temperature is explored in this paper and performs well under simulated conditions. A control strategy for maintaining particle outlet temperature via beam defocusing was also developed and successfully tested on-sun. Other particle receiver designs are also being developed in parallel for particle based CSP applications that do not rely solely on gravitation to feed the particles through the concentrated solar flux [6].

To safely operate the G3P3 pilot facility, while gathering component performance data, the combination of the known control strategies will be utilized. In order to control receiver outlet temperature, two variables can be manipulated, namely receiver mass flow rate and solar heat flux input.

## 2 SOFTWARE AND CONTROLS

The software and controls are written in the graphical programming language LabVIEW, owned by National Instruments. LabVIEW provides a broad selection of tools including modules which can provide various input and output signal processing, temperature measurement (thermocouples and resistance temperature detectors), strain gauges, motion controllers (using different communication protocols; Recommended Standard (RS232) serial ports, or Ethernet IP), and many more.

The G3P3 USA Supervisory Control and Data Acquisition (SCADA) will control and acquire over 1000 signals coming from components located at each level of the tower. Instrumentation boxes are located at each tower level for control and signal acquisition. The signals from each box are fed into the primary SCADA interface.

The SCADA system uses a popular programming architecture, Queue State Machine Architecture (QSMA). Figure 1 shows the general map of the interfaces and the main SCADA software.

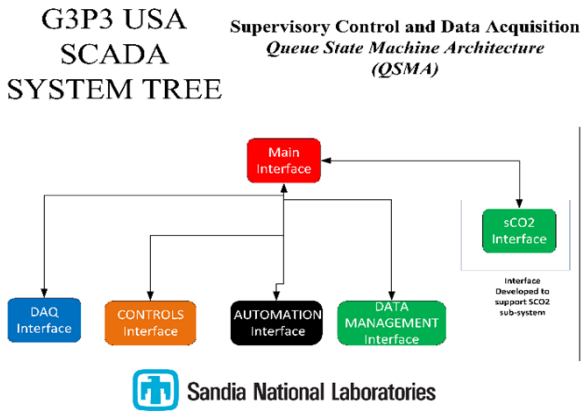


**FIGURE 1**: QSMA DIAGRAM OF THE SCADA

### 2.1 Control Architecture

The architecture consists of two main monitoring loops, the producer loop and consumer loop. The producer loop is triggered when a command is provided in the user interface (UI) window, (e.g. Log DATA). The consumer loop waits for the producer loop to generate an event then executes the command.

The SCADA main interface is composed of five interface sisters: 1) DAQ Interface, 2) CONTROLS interface, 3) AUTOMATION interface, 4) DATA management interface, and 5) sCO2 interface. All interfaces run queue state machine architectures. In this way, operators can communicate through the queue via the producer loop to interface with the data handler system in the consumer loop. This system is composed of N queues running in memory, which all have assigned names so the system can know which queue to access correctly to deliver the correct message.

The benefit of using the queue messaging handle system is that the system can deliver messages and data. The data can be of any type, ranging from a simple double numeric value to a

large array of data points. This enables the user to easily manage a large integrated system. The DAQ interface handles monitoring and data acquisition for each level and sequentially sends the data to the main SCADA interface for the user to visualize the real-time data of each signal.

The CONTROLS interface manages triggering and manipulating any output of the system that will control hardware attached to any functioning component (pumps, slide gate motors, relief valves, etc.). The AUTOMATION interface is in charge of executing the proportional-integral-derivative (PID) controllers, with the functionality to automate different testing campaigns to achieve different data points. This interface also has Machine Learning capabilities to adapt to different testing scenarios, for example, what the influence of ambient wind conditions would be in combination with flux measurements. The DATA MANAGEMENT interface processes all batches of data from DAQ interface, consolidating the data and sending it to the Network Attached Storage (NAS) system for data archival. The $sCO_2$ interface controls the supercritical carbon dioxide heat rejection loop in order to reject the heat that is absorbed from the solar resource. The primary heat exchanger is the interface between the particle process and the $sCO_2$ thermal loop. This system has its own interface, because it is controlled by a separate operator than the main particle loop. Operation of the $sCO_2$ loop is the most unpredictable in nature, therefore the necessary engineered controls, safety interlocks and user-input functionality is needed for safe operation of the equipment.

### 2.2 Data Logging and Archiving

The DAQ and DATA MANAGEMENT interfaces execute the data logging and archival data storage of the overall system. The DAQ interface acquires the signals from the National Instruments hardware, which then sends the data packets through queue messenger handlers to the DATA MANAGEMENT interface. The DATA MANAGEMENT interface processes the data packets and validates the data from each individual level of the tower. If the data contains anomalies or it is incorrect, it will notify the user about a possible incorrect signal from the physical sensor. Once the data has been validated, the DATA MANAGEMENT interface would connect to the NAS.

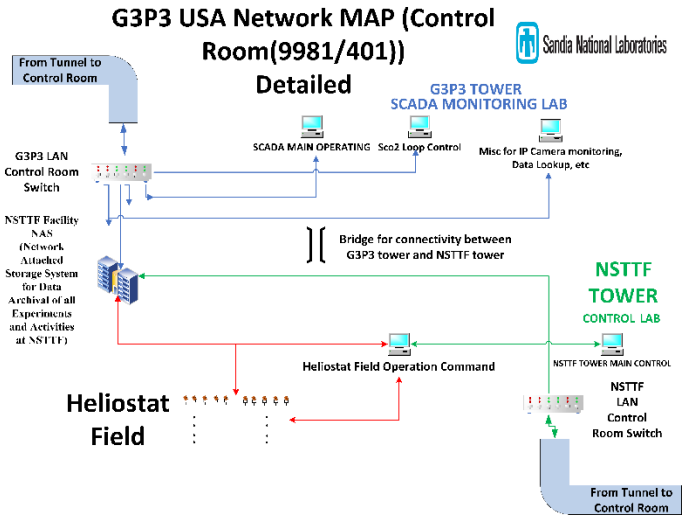


**FIGURE 2**: NAS INTEGRATION WITH THE G3P3 LAN

The NAS system is a six-bay NAS from Synology with 8 GB random-access memory (RAM). Four of the drives would be used for RAID type technology to store and mirror the data to avoid any data loss. The other two SSD's will be used for CACHE memory processing, one for reading and the other for writing. This capability will allow the user to retract and extend data faster than using copy and paste methods. The NAS is connected to a 10 GBps LAN that will interconnect all the rest of the system hardware that require an Ethernet connection. See Figure 2 for the connection of the NAS with all the rest of network-based components.

### 2.3 User Interface

The graphical user interface is a front panel functionality in LabVIEW that allows the user to display indicators and control variables to control the inputs and outputs of National Instruments controlled hardware. The UI is composed of different tabs that are assigned to each level of the new G3P3 tower. The user has the flexibility of changing to a different tab to monitor the specific level of interest. It also has general controls for starting data acquisition and exiting the DAQ interface program. The UI has a simple linear display to provide the user high level details when controlling certain outputs of the system.

LabVIEW includes limited options for animation and graphics for display on the front panel. Most of the buttons and the functionality are designed and pre-defined by LabVIEW internal libraries. The user can integrate other graphical display software with the front panel of the UI for a better representation of the system to match the engineering drawings, such as the piping and instrumentation diagrams (P&ID's).

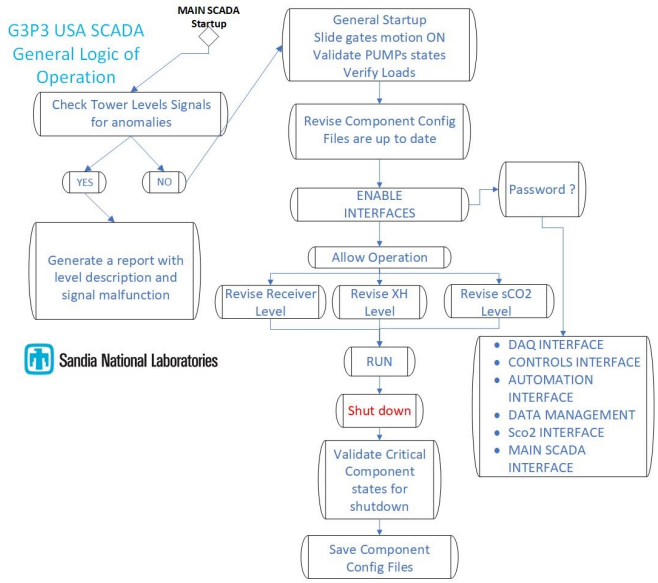


**FIGURE 3**: GENERAL STARTUP OF MAIN INTERFACE OF G3P3 USA SCADA

### 2.4 SCADA Start-Up and Integration

The start-up operation of the main interface of the SCADA system is based on a logical start up, where the main interface is performing different checks and allows the user to continue if all conditions are met. Figure 3 shows how the general start-up of the Main Interface executes and inspects all the levels, then proceeds to validate the configuration files of each sub-system or level of the G3P3 tower. After all the conditions are successfully met, the user can launch the different interfaces mentioned in the Control Architecture section. Once the interfaces are running, the user will revise the conditions of the main critical sub-systems for example the Receiver and the $sCO_2$ system. After the operator is confident with the state of the sub-system, the user can start running the system. This logic map can be extended to customized variables in different test campaigns; for example, mass flow rates above a certain threshold that require additional checks before a different sub-system can be enabled.

## 3 SAFETY INTERLOCKS

During operation, if the $sCO_2$ density is below the threshold of 820 kg/m$^3$ for more than five seconds, the pump should be shut off automatically by the logic in the control system. This is a primary safety feature to protect the bearings of the main circulator pump. Similarly, the pump start option would be disabled if the density threshold is not met.

For pressure safety, an automatic venting feature of the $sCO_2$ loop ensures safe operation. A set value manages the automatic venting between two thresholds. Automatic venting is controlled by the software logic. Hard wired interlocks located at the hardware will also be utilized to ensure safe operation in case of a power failure or loss of communication. The backup power system cannot simultaneously support all system components, therefore, low voltage operated local relays are selected as an alternative to the software interlocks.

## 4 OPERATIONAL PHILOSOPHY

The supercritical carbon dioxide process diagram depicted in Figure 4 shows the overall operation of the G3P3 cooling loop as well as the main components in the $sCO_2$ loop. The particle recirculation loop interacts with the $sCO_2$ loop at the primary heat exchanger (PHX) component, indicated to the right-hand side of the diagram in Figure 4. The primary heat input to the system is concentrating solar heat flux, where the solar flux is directly interacting with the primary heat transport medium (particles) at the FPR. Hot and cold TES bins are integrated into the system to enable nighttime operation of the $sCO_2$ thermal loop. The relative positions of the main particle-side components are illustrated in Figure 5.

### 4.1 Falling Particle Receiver

The function of the FPR is analogous to the combustion process in a conventional power generation facility in that it controls the primary heat input to the process. Heat input in FPR is controlled by regulating the mass flow rate of particles through the FPR with the objective of maintaining a constant receiver outlet temperature in the presence of variable solar flux, ambient temperature, and FPR inlet temperature. In addition to nominal operational control strategies, safety interlocks are implemented to protect from events caused by instrument or equipment failure and automated scheduling is used to provide smooth transitions through start-up, idle, and shutdown periods.

Transient operating conditions can be as result of user-controlled input such as start-up, shut down or change of the operating condition to a different set point. External factors that are not controlled by the user/operator, like cloud overcast, wind conditions, and instrument or equipment failure can also lead to system transient behavior.

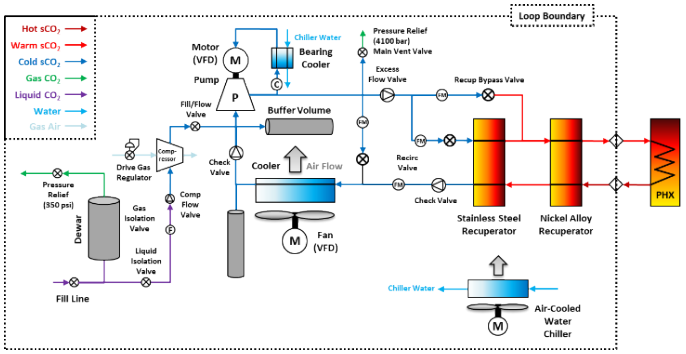


**FIGURE 4**: SUPERCRITICAL CARBON DIOXIDE COOLING LOOP PROCESS DIAGRAM

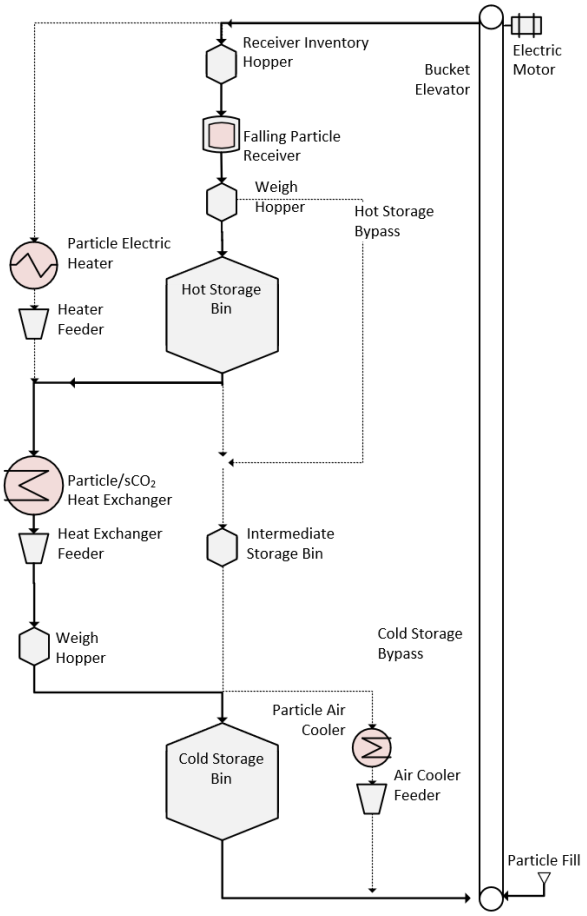


**FIGURE 5**: PARTICLE SIDE RECIRCULATION LOOP PROCESS FLOW DIAGRAM

The mass flow rate corresponds to the particle curtain thickness and subsequently the opaqueness of the heat absorbing particle curtain. Increased particle mass flow rate results in increased particle curtain thickens and vice versa. The particle curtain thickness/mass flow rate have an inverse relationship to the temperature increase across the receiver. For a constant heating power and constant receiver inlet temperature, the mass flow rate dictates the receiver outlet temperature. A higher mass flow rate results in a lower overall temperature increase, which leads to a lower receiver outlet temperature for this operating condition.

Receiver mass flow rate is controlled using a flow control valve. High-temperature solid media flow control valves can utilize a slide gate, linear actuator, and 3-phase motor to control the particle flow area and consequently the particle mass flow rate. The motor is controlled in LabVIEW by sending a digital signal, indicating position, speed, acceleration, deceleration, and move type. An analog feedback signal indicates the motor position following a move. Mass flow rate is discreetly measured by making use of the gravimetric method, taking batch measurements of the particle mass flow. On-sun testing has been performed to prove the effectiveness of the FPR technology and mass flow rate control strategy. In these tests, FPR outlet temperatures were controlled within 10 °C of the setpoint under conditions of variable solar flux, ambient temperature, wind speed, and particle inlet temperature (anticipated disturbance variables). Results from this test campaign are captured in Figure 6.

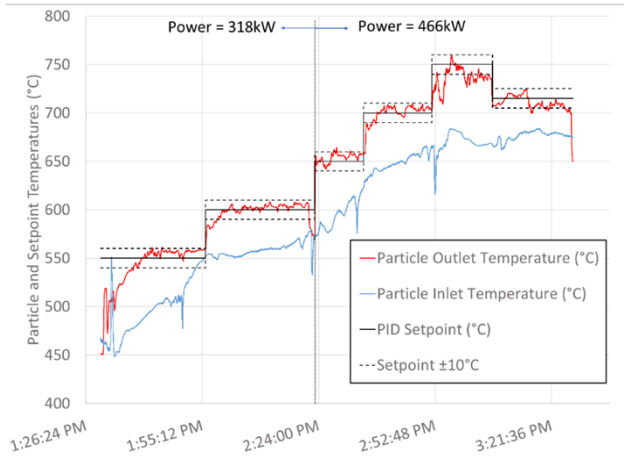


**FIGURE 6**: PARTICLE TEMPERATURE CONTROL TEST ON OCT. 8, 2020 [5]

The mass flow rate corresponds to the particle curtain thickness and subsequently the opaqueness of the heat absorbing particle curtain. Receiver mass flow rate is controlled using a flow control valve. High-temperature solid media flow control valves can utilize a slide gate, linear actuator, and 3-phase motor to control the particle flow area and consequently the particle mass flow rate. The motor is controlled in LabVIEW by sending a digital signal, indicating position, speed, acceleration, deceleration, and move type. An analog feedback signal indicates the motor position following a move. Mass flow rate is discreetly measured by making use of the gravimetric method, taking batch measurements of the particle mass flow.

The local DNI can have substantial fluctuations over sub-hourly intervals, which necessitates disturbance rejection strategies either by orienting the heliostat field to maintain a constant solar flux at the receiver and/or by controlling the receiver mass flow rate. The mass flow rate control strategy is utilized here. Disturbance rejection and reference tracking can be accomplished with a combined feedback and feedforward control action, where feedback PID gains can be designed to maintain a desired FPR outlet temperature. Control strategies are currently being tested on an integrated system model in Simulink, which will be ran in parallel with LabVIEW in real time for model validation and testing purposes.

The two-degree of freedom feedback and feedforward control framework can be designed using a reduced-order lumped model according to a volumetric energy balance over the falling particle curtain. Accounting for absorbed solar irradiation, gray body re-radiation, solid particle advection through the control volume, and convective losses, we have

$$\rho_s c_{p,s} V_s \frac{dT_s}{dt} = \alpha_s G_{solar} - \sigma \epsilon_s A_s \left(T_s^4 - T_\infty^4\right) - 2A_s h_\infty (T_s - T_\infty) - \dot{m} c_p$$

Where we have one state variable, $T_s$, three disturbance inputs, $G_{solar}$, $T_\infty$, and $T_{s,in}$, and one control input, $\dot{m}$. Simplifying this to $\frac{dT_s}{dt} = F(T_s, T_\infty, T_{s,in}, G_{solar}, \dot{m})$, we linearize the model around some moving reference state to obtain the state-space form

$$\frac{dT'_s}{dt} = \beta T'_s + \zeta \dot{m}' + B_w w$$

where

$$B_w = [\gamma \ \theta \ \psi \ 1]$$

$$w = \left[T'_\infty \ T'_{s,in} \ G'_{solar} \ F^0\right]^T$$

and the measured outputs, $z$, are formulated as

$$z = C_z T'_s + D_{zw} w$$

where $C_z$ and $D_{zw}$ are sparse matrices such that

$$z = \left[T'_s \ T'_\infty \ T'_{s,in} \ G'_{solar}\right]^T.$$

The superscript $[\,\cdot\,]'$ indicates a difference between the true and reference variable, $\beta$, $\gamma$, $\theta$, $\psi$, $\zeta$ are the respective partials of $F$, and $F^0$ is the reference time derivative. We can now design a feedback and feedforward controller using the linearized system. We use a simple proportional feedback control law, $\dot{m}'_{fb} = K_p e$, where $e$ is the difference between the measured FPR outlet temperature and the assigned setpoint. The feedback control law is coupled with a dynamic feedforward control law that is designed to reject disturbances from solar irradiation, inlet temperature, and ambient temperature. Specifically, we want to design a dynamic controller, $K_{uw}$, to produce a control input, $\dot{m}'_{ff} = K_{uw} w$, such that the transfer function $T_{wz} := z/w$ is driven to zero. Using this formulation, the resulting dynamic controller is

$$K_{uw} = -\left(\frac{B_w}{\zeta} + \frac{C_z^+ D_{zw}}{\zeta e^{\beta t}}\right)$$

where $C_z^+$ is the Moore-Penrose inverse of $C_z$. The mass flow rate setpoint can then be assigned according to $\dot{m} = \dot{m}_{fb} + \dot{m}_{ff}$. The results from a simulation that utilizes this control methodology are provided in Figure 7. The control logic diagram for the receiver is depicted in Figure 8.

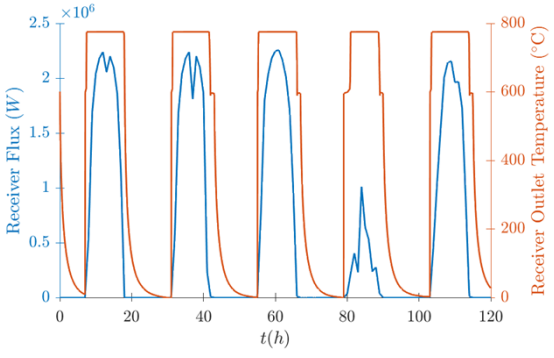


**FIGURE 7**: EXAMPLE SIMULATION RESULTS FOR THE FPR OPERATION UNDER VARIABLE SOLAR FLUX CONDITIONS.

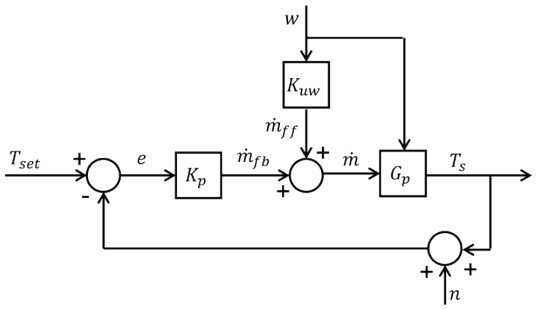


**FIGURE 8**: CONTROL FRAMEWORK DIAGRAM FOR REFERENCE TRACKING AND DISTURBANCE REJECTION AT THE FPR. $G_p$ REPRESENTS THE RECEIVER PLANT AND $n$ IS SIGNAL NOISE IN THE FPR OUTLET TEMPERATURE MEASURMENT.

Practical characteristics of the flow control valve and receiver design lead to constrained operating conditions when solely relying on particle mass flow rate as a control variable. For example, the falling particle curtain can only be reduced to a certain thickness (i.e. opaqueness) before the receiver back wall heat shielding is over-exposed to incident flux and damaged. To increase the particle outlet temperature and avoid back wall damage, particle mass flow rate is stopped at a lower limit while the FPR is being irradiated. In the case that the process control requires receiver outlet temperature to decrease, the receiver mass flow can be gradually increased until the maximum open position is reached. Beyond the maximum mass flow rate, particle outlet temperature can only be decreased by removing solar input power. These practical limitations of the flow control valve and receiver provide limited temperature modulation capability when solely altering the receiver mass flow rate, making solar flux control an important control variable to extend the operational domain of this system in future work.

Solar flux input as a control variable has very little practical limitation in terms of modulating power. A range of 0 % to < 100 % of the rated thermal duty of G3P3 is possible. The main control technique is to utilize the required power level specified by the operator for a given operating condition. This is accomplished by selecting the number of heliostats required. Operational capability of the heliostat field includes pre-selecting the heliostat group that is required for the next operational set point. Movement and response time of the heliostats is very short, on the order of 2 seconds after the operator provides the command signal.

### 4.2 Thermal Energy Storage

The primary function of the thermal energy storage system is to store thermal energy for later use and the secondary function is to facilitate inventory management. At normal operating conditions, high temperature particles are fed from the receiver to the high temperature storage bin. A hot storage bypass line enables functionality for ramp-up, idle, and shutdown operations. Logic in the control system determines when the filling of the hot storage bin can commence. Particles from the

hot storage feeds into the PHX during steady state discharge operation. Heat attenuation in the particles during the charge, hold, and discharge phases causes a transient outlet temperature profile that can cause large temperature differentials in the discharge phase, demonstrated in Figure 9, which is an example result produced by a model that was developed to capture the particle flow and heat transfer in flat-bottomed granular storage bins. The modeled transient bulk temperature of particles at the storage bin outlet was first described and verified with experimental results in [7].

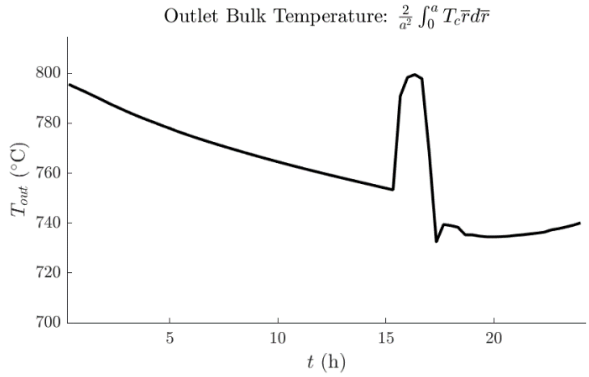


**FIGURE 9**: EXAMPLE OF THE TRANSIENT OUTLET PROFILE IN THE HOT PARTICLE STORAGE BIN

A 200 kW electrical resistance heater bank is located at the outlet of the hot storage bin in order to smooth out the characteristic outlet profile for brief periods of time when the outlet temperatures may dip below requirements. In addition to outlet controls, the interior wall temperature of the bins will be maintained during non-operational times by electric resistance heaters. Thermocouples will be embedded between the refractory insulation layers to indicate when electric heating is necessary.Cold storage hardware functions as an inventory storage vessel during the steady state discharging process. For certain operating conditions, the cold storage bypass line feeds particles directly to the elevator system in case the particle temperature upstream of the cold storage bin is outside the required operating range. This can also be used during the pre-heating of selected components.

### 4.3 Primary Heat Exchanger

Being the interfacing component between the particle side and the $sCO_2$ loop, the PHX is exposed to a wide variety of thermal transient conditions. During a change in set point, start-up or shut down, a thermal transient over time is typical to observe. In addition to the thermal transient over time, a spatial thermal transient will exist across the PHX.

Particle mass flow control through the heat exchanger, which is the primary source of heat input, is achieved by utilizing a proportionally controlled slide gate. Feedback signals from temperature sensors are fed into a PID control algorithm to control the mass flow through the heat exchanger with the objective of maintaining desired particle and $sCO_2$ outlet temperatures. Feedforward control strategies can also be applied to improve performance, as was demonstrated in [8]. Since the upstream equipment and particle recirculation loop have the functionality to isolate receiver operation from PHX operation, the particle mass flow rate operational range can practically be varied from 0 % to 100 %. The heat rejection is controlled by the mass flow rate of $sCO_2$ through the PHX, rejecting the heat to the ambient environment.

### 4.4 $sCO_2$ Thermal Loop

The operational philosophy for the $sCO_2$ loop for the G3P3 system is heavily based on experience acquired during the operation of Sandia's SuNLaMP FPR [1], [9], [10]. The $sCO_2$ loop and PHX control has been attained by establishing a balance at the PHX to provide enough $sCO_2$ cooling and flow of particles to avoid damaging any of the equipment. The $sCO_2$ and particle flow through the heat exchanger is expected to be managed by two separate control subsystems: PHX particle flow subsystem and $sCO_2$ flow subsystem.

### 4.5 Electrical Heaters

Electrical heaters would be utilized for trim heating to be able to fine-tune the operation at steady state. Pre-heating of equipment also utilize electrical heating elements to pre-heat thermal expansion sensitive components.

## 5 CONCLUSION

Operations, as presented here, of a particle-based CSP process is analogous to a conventional power generation plant, but the primary heat transport medium in the form of solid particles requires novel operational controls. Strategies to control the temperatures, mass flow rates, and power through the system is based on operational experiences and lessons learned from on-sun testing at the NSTTF. Ground based electrically heated testing was also used to gain experimental experience with the particle-$sCO_2$ heat exchangers and auxiliary components.


## ACKNOWLEDGEMENTS

Department of Energy Solar Energy Technologies Office under Award Number 34211. Sandia National Laboratories is a multimission laboratory managed and operated by National Technology & Engineering Solutions of Sandia, LLC, a wholly owned subsidiary of Honeywell International Inc., for the U.S. Department of Energy's National Nuclear Security. Administration under contract DE-NA0003525. SANDXXXX


## REFERENCES


[1] M. D. Carlson, K. J. Albrecht, C. K. Ho, H. F. Laubscher, and F. Alvarez, "High-Temperature Particle Heat Exchanger for sCO2 Power Cycles," Albuquerque, 2020. doi: https://doi.org/10.2172/1817287.

[2] K. J. Albrecht, H. F. Laubscher, M. D. Carlson, and C. K. Ho, "Development and testing of a 20 KW moving packed-bed particle-to-SCO2 heat exchanger and test facility," *Proc. ASME 2021 15th Int. Conf. Energy Sustain. ES 2021*, pp. 1–6, 2021, doi: 10.1115/ES2021-64050.

[3] B. H. Mills, C. K. Ho, N. R. Schroeder, R. Shaeffer, H. F. Laubscher, and K. J. Albrecht, "Design Evaluation of a Next-Generation High-Temperature Particle Receiver for Concentrating Solar Thermal Applications," *Energies*, vol. 15, no. 5, 2022, doi: 10.3390/en15051657.

[4] C. K. Ho, "A review of high-temperature particle receivers for concentrating solar power," *Appl. Therm. Eng.*, vol. 109, pp. 958–969, 2016, doi: 10.1016/j.applthermaleng.2016.04.103.

[5] C. K. Ho *et al.*, "Receiver design and On-Sun testing for G3P3-USA," in *AIP Conference Proceedings*, 2022, vol. 2445. doi: 10.1063/5.0086071.

[6] M. Ebert *et al.*, "Operational experience of a centrifugal particle receiver prototype," in *AIP Conference Proceedings*, 2019, vol. 2126, no. July. doi: 10.1063/1.5117530.

[7] K. Plewe, J. N. Sment, M. J. Martinez, C. K. Ho, and D. Chen, "Transient thermal performance of high-temperature particle storage bins," in *AIP Conference Proceedings*, 2022, vol. 2445. doi: 10.1063/5.0085649.

[8] M. Fernández-Torrijos, K. J. Albrecht, and C. K. Ho, "Dynamic modeling of a particle/supercritical CO2 heat exchanger for transient analysis and control," *Appl. Energy*, vol. 226, no. March, pp. 595–606, 2018, doi: 10.1016/j.apenergy.2018.06.016.

[9] K. J. Albrecht and C. K. Ho, "High-temperature flow testing and heat transfer for a moving packed-bed particle/sCO2 heat exchanger," in *AIP Conference Proceedings*, 2018, vol. 2033. doi: 10.1063/1.5067039.

[10] K. J. Albrecht, M. D. Carlson, and C. K. Ho, "Integration, control, and testing of a high-temperature particle-to-sCO2 heat exchanger," in *AIP Conference Proceedings*, Jul. 2019, vol. 2126, no. 1, p. 30001. doi: 10.1063/1.5117513.